Exchange carrier-carrier scattering of photoexcited spin-polarized carriers in GaAs quantum wells: Monte Carlo study

Antónia Mošková and Martin Moško
Institute of Electrical Engineering, Slovak Academy of Sciences, Dúbravská cesta 9, 842 39 Bratislava, Slovakia
(Received 1 March 1993; revised manuscript received 6 October 1993)

Thermalization of near-band-gap excited carriers in an intrinsic GaAs quantum well is studied using ensemble Monte Carlo simulation. Carrier-carrier interaction is treated like two-particle collisions due to the screened Coulomb interaction. The indistinguishability of two colliding electrons (holes) is included by taking into account the exchange electron-electron (hole-hole) scattering between the electrons (holes) of like spin. The model is modified to the case of spin-polarized carriers. We show that the thermalization of the spin-polarized carriers is several times slower than the thermalization of the spin-randomized ones when the carrier density exceeds 10^{11} cm^{-2}. The effect is due to the exchange scattering, which significantly weakens the direct Coulomb scattering in the dense carrier gas. For small densities the exchange becomes negligible. Possibilities to observe the exchange experimentally are discussed.

I. INTRODUCTION

When two electrons or holes of like spin collide, the direct Coulomb scattering between them is weakened by the exchange scattering[1,2] which is a quantum effect arising from the particle indistinguishability. Femtosecond pump-probe spectroscopy of the GaAs crystals[3] and quantum wells[4,5] leads to observation of the thermalization of the nonthermal electron-hole (*e-h*) plasma by *e-e*, *e-h* and *h-h* scattering,but there was no attempt to isolate the exchange effect in the *e-e* and *h-h* collisions.

In numerous Monte Carlo (MC) simulations of carrier-carrier scattering, the exchange was either ignored[6–13] or overestimated by completely neglecting the collisions between the carriers of like spin.[14,15] Wingreen and Combescot[16] have shown that the exchange is negligible in the nondegenerate limit. However, at very high electron concentrations, molecular-dynamics-coupled MC simulations[17,18] demonstrate the reduction of the *e-e* interaction due to the exchange effect. Recently,[19] we have included the exchange effect into the traditional (Fermi-golden-rule-based) MC simulation. About a 30% reduction of the *e-e* scattering rate in the GaAs quantum well was found for a sheet electron density of 1.5×10^{11} cm^{-2} at 77 K and at mean electron energies not very far from equilibrium.

In this work, we present MC simulation of the thermalization of the *e-h* plasma excited into the intrinsic GaAs quantum well.[4,5] The exchange scattering is included by deriving the *e-e* and *h-h* scattering rates from Fermi's golden rule for indistinguishable particles. Unlike the above-cited experiments and calculations, which deal with spin-randomized (SR) plasma, we also study the thermalization of the spin-polarized (SP) plasma. In the SP plasma each *e-e* (*h-h*) collision occurs between the electrons (holes) of like spin and the effect of exchange is, therefore, more important than in the SR plasma. We find that the thermalization of the SP plasma is several times slower than the thermalization of the SR plasma when the density of the *e-h* pairs exceeds 10^{11} cm^{-2}. This pronounced difference tends to disappear with decreasing carrier density. The effect is due to the exchange which significantly weakens the *e-e* and *h-h* Coulomb interactions in the dense SP plasma. We discuss a chance to detect the exchange by comparative measurements of the thermalization of SP (Ref. 20) and SR (Refs. 4 and 5) plasmas.

In Sec. II we discuss the MC model. In Sec. III we show numerical results for an isolated electron gas and in Sec. IV we extend the discussion to an interacting *e-h* plasma. Concluding remarks are given in Sec. V.

II. TRANSPORT MODEL AND SIMULATION PROCEDURE

We assume that photoexcited electrons and holes occupy the lowest electron and heavy-hole subband in a rectangular 10-nm GaAs quantum well. The hole generation within the light-hole subbands is neglected assuming the photoexcitation is close to the band gap.[4,5] Effective-mass approximation and sine-envelope function are used to describe the electron and hole quantum states. Carrier-polar optic-phonon scattering is taken into account using conventional MC.[15] Carrier-acoustic phonon interaction is modeled assuming elastic scattering.[21] Its presence in the simulation is in fact unimportant because elastic scattering does not contribute to the relaxation of the energy distribution. Due to the same reason, we entirely neglect ionized impurity scattering. In what follows, we discuss carrier-carrier scattering.

An electron or a hole changes its in-plane wave vector from $\mathbf{k}$ to $\mathbf{k}'$ by collision with another electron or hole, which is scattered from $\mathbf{k}_0$ to $\mathbf{k}_0'$. The probability of such scattering is given by Fermi's golden rule as

$$S_{\mathbf{k},\mathbf{k}_0\to\mathbf{k}',\mathbf{k}_0'}=\frac{2\pi}{\hbar}M^2\delta[\varepsilon(\mathbf{k})+\varepsilon(\mathbf{k}_0)-\varepsilon(\mathbf{k}')-\varepsilon(\mathbf{k}_0')]\ , \quad (1)$$

where $\varepsilon(\mathbf{k})$ is the carrier energy and M^2 is the square of the scattering amplitude. Taking

$$M^2=|M_{\mathbf{k},\mathbf{k}_0\to\mathbf{k}',\mathbf{k}_0'}|^2\ , \quad (2)$$

0163-1829/94/49(11)/7443(10)/$06.00

where

$$M_{\mathbf{k},\mathbf{k}_0\to\mathbf{k}',\mathbf{k}_0'}\equiv\langle\mathbf{k}',\mathbf{k}_0'|W|\mathbf{k},\mathbf{k}_0\rangle$$

is the matrix element for the screened Coulomb energy W of the colliding carriers, it is implicitly assumed that the scattering $\mathbf{k}\to\mathbf{k}'$, $\mathbf{k}_0\to\mathbf{k}_0'$ is distinguishable from the exchange scattering $\mathbf{k}\to\mathbf{k}_0'$, $\mathbf{k}_0\to\mathbf{k}'$. This is correct, to a good approximation,[22] for e-h scattering. For e-e and h-h scattering, the colliding particles are indistinguishable and exchange scattering modifies M^2 as follows.[1] When electrons or holes with parallel spins collide, the interference occurs between the matrix element $M_{\mathbf{k},\mathbf{k}_0\to\mathbf{k}',\mathbf{k}_0'}$ and the "exchange" matrix element $M_{\mathbf{k},\mathbf{k}_0\to\mathbf{k}_0',\mathbf{k}'}$. Then, instead of (2), one has to take

$$M_p^2=|M_{\mathbf{k},\mathbf{k}_0\to\mathbf{k}',\mathbf{k}_0'}-M_{\mathbf{k},\mathbf{k}_0\to\mathbf{k}_0',\mathbf{k}'}|^2 .$$

When the spins are antiparallel, the interference does not occur and

$$M_a^2=|M_{\mathbf{k},\mathbf{k}_0\to\mathbf{k}',\mathbf{k}_0'}|^2+|M_{\mathbf{k},\mathbf{k}_0\to\mathbf{k}_0',\mathbf{k}'}|^2 .$$

Introducing the probability p that the spins of colliding electrons (holes) are parallel, the "averaged" square of the scattering amplitude reads

$$M^2=\tfrac{1}{2}\{p|M_{\mathbf{k},\mathbf{k}_0\to\mathbf{k}',\mathbf{k}_0'}-M_{\mathbf{k},\mathbf{k}_0\to\mathbf{k}_0',\mathbf{k}'}|^2 +(1-p)(|M_{\mathbf{k},\mathbf{k}_0\to\mathbf{k}',\mathbf{k}_0'}|^2+|M_{\mathbf{k},\mathbf{k}_0\to\mathbf{k}_0',\mathbf{k}'}|^2)\} , \quad (3)$$

where $p=\frac{1}{2}$ for SR plasma, $p=1$ for SP plasma, and the extra factor of $\frac{1}{2}$ is justified in the discussion of Eq. (4).

The e-e (h-h) scattering rate based on (3) can be calculated in a similar way like the rates without exchange.[14] First we calculate the pair scattering rate

$$\lambda(|\mathbf{k}-\mathbf{k}_0|)=N_S A\sum_{\mathbf{k}',\mathbf{k}_0'}S_{\mathbf{k},\mathbf{k}_0\to\mathbf{k}',\mathbf{k}_0'} , \quad (4)$$

where N_S is the electron (hole) sheet density and A is the normalization area for the plane waves $|\mathbf{k}\rangle$. Since for M^2 given by (3) we have

$$S_{\mathbf{k},\mathbf{k}_0\to\mathbf{k}',\mathbf{k}_0'}=S_{\mathbf{k},\mathbf{k}_0\to\mathbf{k}_0',\mathbf{k}'} ,$$

summation in (4) leads to double counting of each transition. To avoid this, the factor of $\frac{1}{2}$ was introduced into (3). The matrix element $M_{\mathbf{k},\mathbf{k}_0\to\mathbf{k}',\mathbf{k}_0'}$ is given as[7,14,15]

$$M_{\mathbf{k},\mathbf{k}_0\to\mathbf{k}',\mathbf{k}_0'}=\frac{1}{A}\delta_{\mathbf{k}+\mathbf{k}_0,\mathbf{k}'+\mathbf{k}_0'}\frac{-e^2H(Q)}{2\epsilon_s Q\epsilon(Q)} , \quad (5)$$

where $Q=|\mathbf{k}-\mathbf{k}'|=|\mathbf{k}_0'-\mathbf{k}_0|$, ϵ_s is the static permittivity, and $\epsilon(Q)$ is the screening function (specified below). The form factor

$$H(Q)=\int dz\int dz_0\phi^2(z)\phi^2(z_0)e^{-Q|z-z_0|} , \quad (6)$$

where $\phi(z)$ is the (sine) envelope function [$H(Q)$ is computed like in our previous work[15]].

Performing the summation in (4) (Ref. 23) one gets

$$\lambda(|\mathbf{k}-\mathbf{k}_0|)=\frac{N_s e^4 m}{8\pi\epsilon_s^2\hbar^3}\int_0^{2\pi}d\varphi\left\{\frac{H^2(Q)}{Q^2\epsilon^2(Q)}+\frac{H^2(Q')}{Q'^2\epsilon^2(Q')} -2p\frac{H(Q)H(Q')}{Q\epsilon(Q)Q'\epsilon(Q')}\right\} , \quad (7)$$

where

$$Q(\varphi)=|\mathbf{k}-\mathbf{k}_0|\sin\left[\frac{\varphi}{2}\right] ,$$
$$Q'(\varphi)=|\mathbf{k}-\mathbf{k}_0|\left|\cos\left[\frac{\varphi}{2}\right]\right| , \quad (8)$$

φ is the scattering angle between the vectors $\mathbf{g}\equiv\mathbf{k}-\mathbf{k}_0$ and $\mathbf{g}'\equiv\mathbf{k}'-\mathbf{k}_0'$, and m is the effective mass ($m=m_e=0.067m_0$ for electrons, $m=m_h=0.44m_0$ for heavy holes). The third term on the right-hand side of (7) describes the exchange e-e (h-h) scattering.

The e-h pair scattering rate is obtained in a similar way, but $S_{\mathbf{k},\mathbf{k}_0\to\mathbf{k}',\mathbf{k}_0'}$ in (4) is expressed through (2). The result is

$$\lambda(|\mathbf{k}-\mathbf{k}_0|)=\frac{N_s e^4\mu}{8\pi\epsilon_s^2\hbar^3}\int_0^{2\pi}d\varphi\frac{2H^2(Q)}{Q^2\epsilon^2(Q)} , \quad (9)$$

where $\mu=2m_e m_h/(m_e+m_h)$, N_s is the hole sheet density, $Q(\varphi)$ is given by (8), and φ is the scattering angle between the vectors $\mathbf{g}\equiv\mu(\mathbf{k}/m_e-\mathbf{k}_0/m_h)$ and $\mathbf{g}'\equiv\mu(\mathbf{k}'/m_e-\mathbf{k}_0'/m_h)$. For the h-e scattering, the "hole variables" in (9) have to be replaced by the "electron variables" and vice versa. Expression (9) is not reduced to (7) when electrons and holes are considered as identical particles. This is due to the omission of the exchange e-h scattering, which is negligible in GaAs.[22] If one neglects the exchange term in (7), then (7) and (9) become identical for $m_e=m_h=m$. (This would not be the case if the matrix elements for e-h and h-h scattering would be derived more precisely, including overlap integrals for the Bloch functions.[24] To our knowledge, such a derivation is still missing for quantum wells in the literature.)

In the approximation of static screening[12,25,26]

$$\epsilon(Q)=1+g_e\left[\frac{e^2m_e}{4\pi\epsilon_s\hbar^2}\right]\frac{f_e(\mathbf{k}=0)}{Q} +g_h\left[\frac{e^2m_h}{4\pi\epsilon_s\hbar^2}\right]\frac{f_h(\mathbf{k}=0)}{Q} , \quad (10)$$

where g is the spin-degeneracy factor and $f(\mathbf{k})$ is the distribution function for electrons (e) and holes (h). In case of heavy holes, static-screening approximation (10) is reasonable for e-h and h-h interactions.[24] Screening of e-e interaction is, however, strongly overestimated by (10) due to the heavy-hole contribution. Holes have to give zero contribution to the dynamic screening of the e-e interaction for $m_h\to\infty$. Static screening (10) does not obey this requirement and gives a much stronger screening of the e-e interaction by holes than by electrons during the

thermalization, because $m_h \gg m_e$. This is not reasonable, because heavy holes can hardly follow fast changes of electron positions. Therefore, for *e-e interaction we use expression (10) without the third term on its right-hand side.* With this screening model we find simulation results (not shown here) close to those obtained for near-band-gap excited plasma with dynamic screening (Fig. 1 in Ref. 12). Similar improvements of static screening were reported for bulk GaAs.[27] Therefore, we believe that the inclusion of dynamic screening would not significantly modify our quantitative analysis of the exchange.

The carrier-carrier scattering rate of a carrier of wave vector $\mathbf{k}$, $\lambda^{c-c}(\mathbf{k})$, is given as

$$\lambda^{c-c}(\mathbf{k})=\frac{1}{N}\sum_{i=1}^{N}\lambda(|\mathbf{k}-\mathbf{k}_{0_i}|)\ , \tag{11}$$

where i is the particle index and N is the number of simulated electrons [for $\lambda^{e-e}(\mathbf{k})$ and $\lambda^{h-e}(\mathbf{k})$] or holes [for $\lambda^{h-h}(\mathbf{k})$ and $\lambda^{e-h}(\mathbf{k})$]. The rates $\lambda^{c-c}(\mathbf{k})$ are implemented into the MC simulation through the following rejection technique.[15]

Instead of (11) we consider the two times lower scattering rate

$$\lambda^{c-c}(\mathbf{k})=\frac{1}{2}\frac{1}{N}\sum_{i=1}^{N}\lambda(|\mathbf{k}-\mathbf{k}_{0_i}|)\ . \tag{12}$$

Replacing the integrands in (7) and (9) by the constant

$$C_{\max}=2\left[g_e\left[\frac{e^2m_e}{4\pi\epsilon_s\hbar^2}\right]f_e(k=0)+g_h\left[\frac{e^2m_h}{4\pi\epsilon_s\hbar^2}\right]f_h(k=0)\right]^{-2}, \tag{13}$$

which is greater than the integrands, we obtain from (12) constant scattering rates

$$\Gamma^{c-c}=\frac{1}{2}\frac{N_s e^4 m}{4\epsilon^2\hbar^3}C_{\max} \tag{14}$$

for *e-e* and *h-h* scattering and a similar expression (with m replaced by μ) for *e-h* scattering. The scattering rate Γ^{c-c} is used in the normal MC framework[15,28] together with electron-phonon scattering rates. When the free flight of the simulated carrier (of wave vector $\mathbf{k}$) is interrupted and the carrier-carrier scattering channel is selected, we select a scattering partner of wave vector $\mathbf{k}_0$ at random from the ensemble. Then we select the angle φ at random between 0 and 2π, we calculate the integrand in (7) [or in (9), when the *e-h* collision takes place], and we test the inequality

$$rC_{\max} < \text{integrand}\ , \tag{15}$$

where r is a random number between 0 and 1. If (15) is fulfilled, the collision as well as the angle φ are accepted and new wave vectors, $\mathbf{k}'$ and $\mathbf{k}_0'$, are computed from the energy and momentum conservation laws.[14,15] If (15) is not fulfilled, the collision is rejected and self-scattering occurs (we put $\mathbf{k}'=\mathbf{k}$ and $\mathbf{k}_0'=\mathbf{k}_0$).

Without the factor of $\frac{1}{2}$ in (12), the artificial overestimation of the carrier-carrier scattering rate would appear in the simulation, because each carrier from the simulated ensemble is scattered not only according to its own scattering probability but also when it is chosen as a scattering partner. When the rate (12) is used instead of (11), the above rejection technique ensures that simulated carriers are effectively scattered with scattering rate (11).[15]

To include Fermi statistics, the final carrier state after the collision, $\mathbf{k}_f$, is accepted, if $f(\mathbf{k}_f)$ is less than a number randomly chosen between 0 and 1. Otherwise, the collision is rejected. To calculate $f(\mathbf{k})$ we proceed as follows.[28] In the two-dimensional (2D) $\mathbf{k}$ space, a grid is set up with mesh cells of the area $\Delta k_x \Delta k_y$ ($\Delta k_x=\Delta k_y=10^4$ cm^{-2}). The maximum occupation number of a cell, allowed by the Pauli exclusion principle, can be expressed as[28]

$$N_p=\frac{g}{(2\pi)^2}\Delta k_x \Delta k_y \frac{N}{N_s}\ . \tag{16}$$

The distribution function $f(\mathbf{k})$ in the whole grid is computed using the relation $f(\mathbf{k})=n(\mathbf{k})/N_p$, where $n(\mathbf{k})$ is the number of electrons (holes) in a cell and $\mathbf{k}$ is the cell center position. For sufficiently small area $\Delta k_x \Delta k_y$ and for $N_p \gg 1$, $f(\mathbf{k})$ is a good occupation number for any state $\mathbf{k}$ inside the cell [our choice of $\Delta k_x \Delta k_y$ ensures a relaxation towards the Fermi function even for the most degenerate distribution (see Fig. 3 in the next section) and a more fine discretization does not change the results]. In (10) and (16) one has $g_e=g_h=2$ for the SR *e-h* plasma, but $g_e=g_h=1$ for the SP *e-h* plasma due to the spin alignment.

In the simulation, photoexcited electrons and holes start their motion from Gaussian energy distributions.[4,5] $f_e(\mathbf{k})$, $f_h(\mathbf{k})$ and $\epsilon(Q)$ are recalculated after short time steps Δ_t.

III. EXCHANGE EFFECTS IN AN ISOLATED ELECTRON GAS

First we study the effect of the exchange scattering on the thermalization of an isolated electron gas, i.e., we neglect the presence of photoexcited heavy holes. This enables us to isolate exchange effects in a most ideal system, in the gas of indistinguishable particles. We start the simulations with an initial Gaussian energy distribution centered at 0.02 eV with a half width of 0.01 eV.[4,5] The MC time step Δ_t is 5 fs and $N=14\,400$. We plot the calculated energy-distribution function normalized like the occupation number $f_e(\varepsilon_e)$ or like the so-called total occupancy $g_e f_e(\varepsilon_e)$.

In Fig. 1 we show the total occupancy $g_e f_e(\varepsilon_e)$ versus time t for three different sheet densities of photoexcited electrons. Only *e-e* scattering is taken into account. For each sheet density, the thermalization of the initial Gaussian energy distribution towards quasiequilibrium Fermi distribution is slower for the SP electron gas (dashed lines) than for the SR electron gas (solid lines). The most pronounced difference between the thermalization rates of the SP and SR electron gases is found for

$N_s = 3.5 \times 10^{11}$ cm^{-2} (to compare the thermalization rates we compare the times necessary for the disappearance of the initial Gaussian peak). The difference between the thermalization rates becomes smaller with decreasing sheet electron density.

To demonstrate the origin of this difference, Fig. 2 shows the same results as Fig. 1, but without the exchange effect. More precisely, the results in Fig. 2 are obtained by omitting the third term in the integrand on the right-hand side of (7). Clearly, without the exchange effect the SP electron gas is thermalized within almost the same time as the SR gas. The slightly slower thermalization of the SP gas at the highest sheet density is due to the Pauli exclusion principle: Since $g_e = 1$, the $\mathbf{k}$ space is available to the two times lower number of electrons and final electron states after the *e-e* collisions, $\mathbf{k}'$ and $\mathbf{k}'_0$, are blocked with higher probability than in the case of the SR gas.

[Since the initial $f_e(\varepsilon_e)$ is generated from the analytical Gaussian function using random numbers, small statistical deviations from the analytical function $f_e(\varepsilon_e)$ appear. Due to these deviations, about 3% greater peak value than one appeared in Figs. 1–3 for $N_s = 3.5 \times 10^{11}$ cm^{-2}. This small error disappears within several femtoseconds and can no longer appear due to the application of the Pauli exclusion principle.]

In Fig. 3, occupation number $f_e(\varepsilon_e)$ versus time t is shown for $N_s = 3.5 \times 10^{11}$ cm^{-2}. The thermalization without electron-phonon interaction (*e-e* only) is compared with the thermalization at 77 and 300 K, when electron-phonon interaction is included. The occupation numbers converge to the quasiequilibrium Fermi-distribution functions (the curves labeled by *F*) which are calculated as follows. Quasi-Fermi energy is obtained from the condition

$$N_s = g_e (2\pi)^{-2} \int d\mathbf{k} f_e(\mathbf{k}) ,$$

with $f_e(\mathbf{k})$ taken as the Fermi function. The electron temperature in the Fermi function is equal to the lattice temperature when electron-phonon interaction is considered. When only the *e-e* interaction is considered, the electron temperature is obtained by numerically solving the equation

$$\langle \varepsilon_e \rangle = g_e (2\pi)^{-2} \int d\mathbf{k} \varepsilon_e(\mathbf{k}) f_e(\mathbf{k}) ,$$

where the mean electron energy $\langle \varepsilon_e \rangle$ is determined by the initial Gaussian distribution and $f_e(\mathbf{k})$ is taken as the Fermi function.

At 300 K, as time progresses, electrons are "pumped" into the high-energy tail of the distribution. This is due to the optical-phonon absorption because the emission is

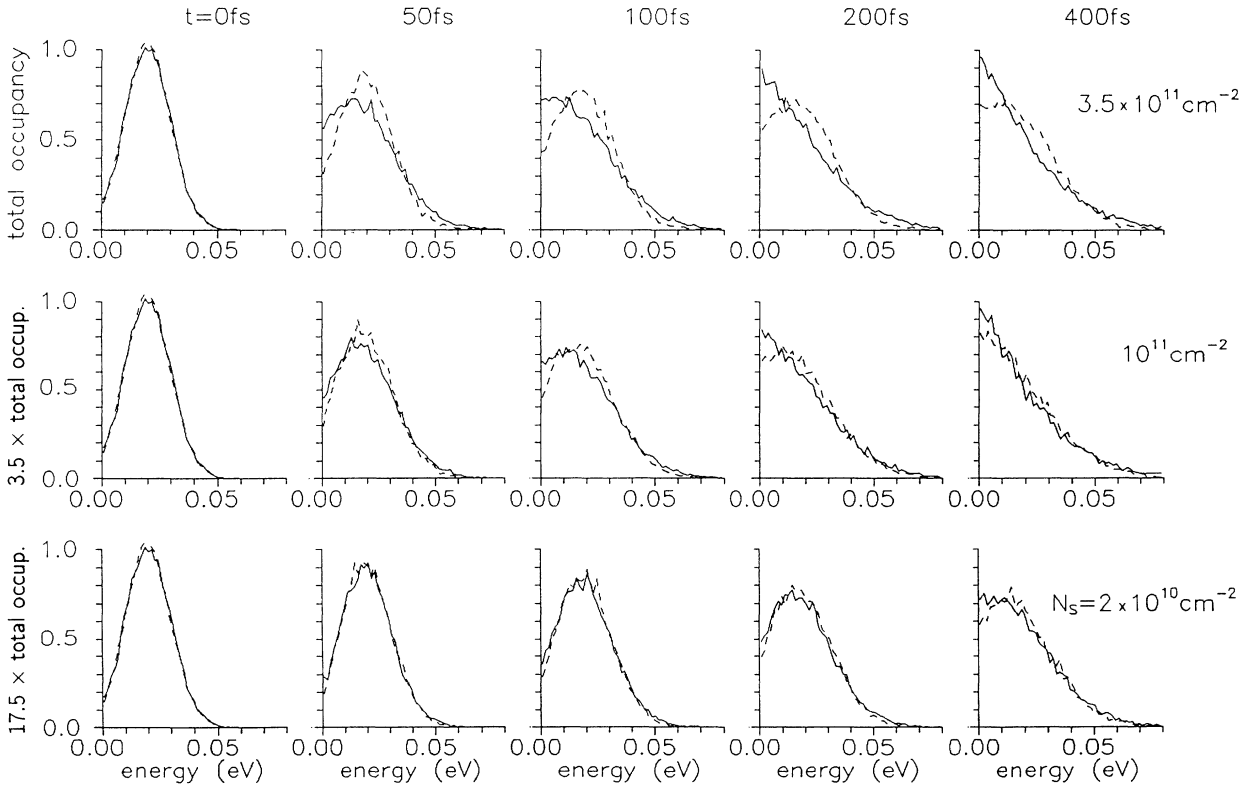

FIG. 1. Total electron occupancy $g_e f_e(\varepsilon_e)$ as a function of electron energy at time instants 0, 50, 100, 200, and 400 fs for sheet electron densities $N_s = 2 \times 10^{10}$, 10^{11}, and 3.5×10^{11} cm^{-2}. Solid curves are for the spin-randomized electron gas ($g_e = 2$), dashed curves are for the spin-polarized electron gas ($g_e = 1$). The initial Gaussian distribution is centered at 0.02 eV with a 0.02 spread. Only *e-e* scattering is taken into account. Distributions for $N_s = 10^{11}$ and 2×10^{10} cm^{-2} are scaled by factors of 3.5 and 17.5, respectively. At the highest sheet density, the initial peak is thermalized within about 400 fs when the gas is spin-polarized, but within 100 fs in the other case.

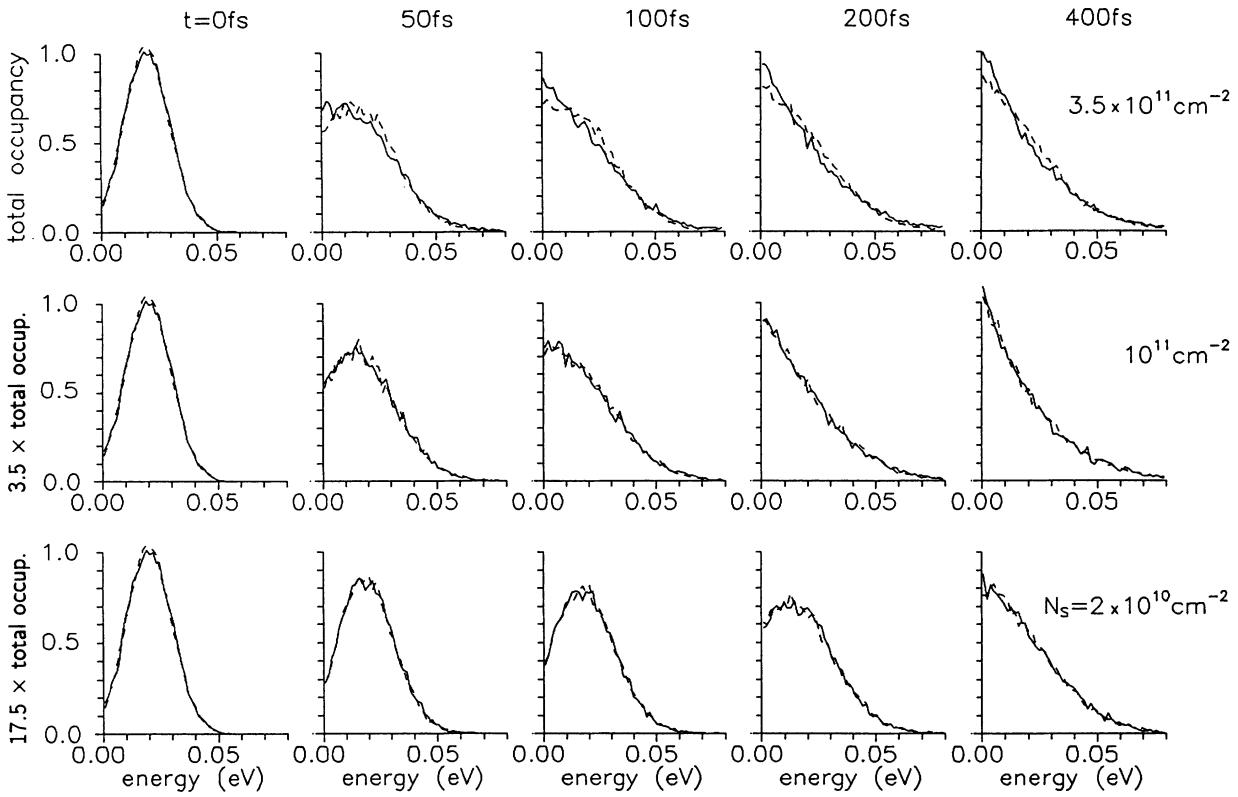

FIG. 2. The same as in Fig. 1, except that *e-e* scattering is taken into account without the exchange effect.

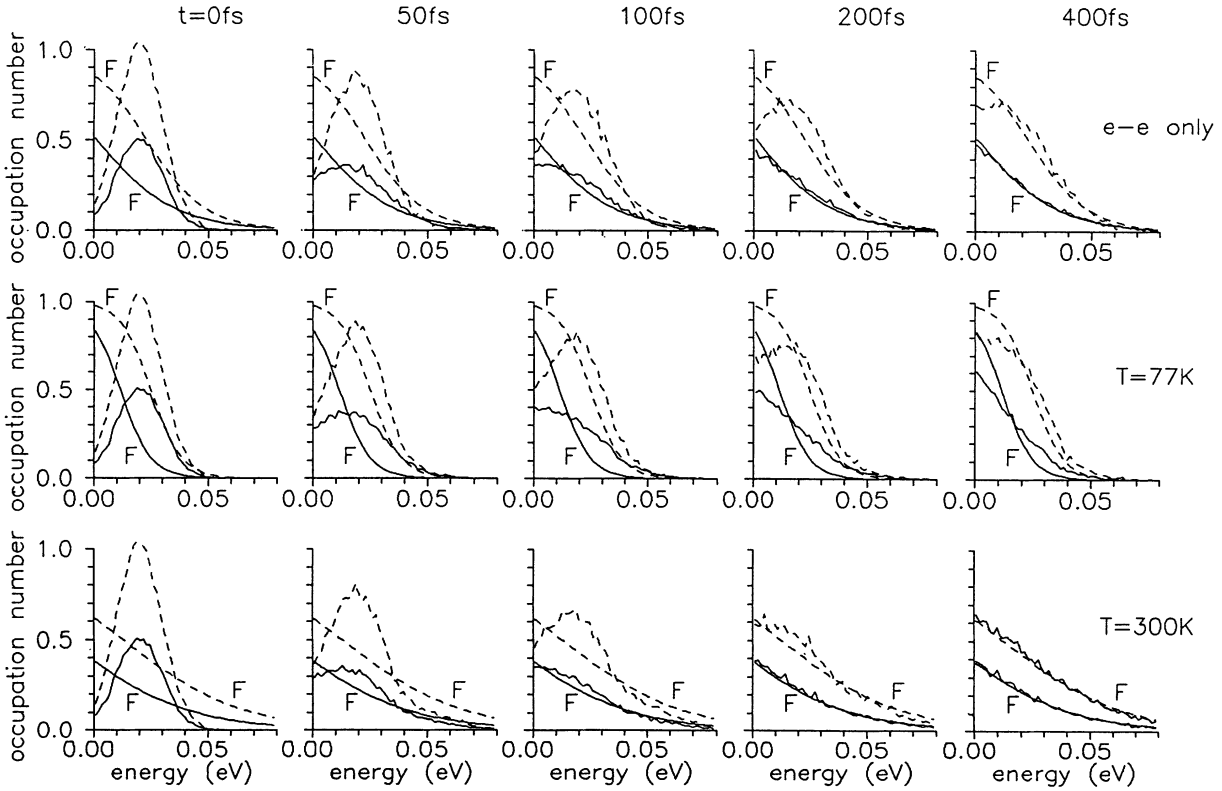

FIG. 3. Occupation number $f_e(\varepsilon_e)$ as a function of electron energy at time instants 0, 50, 100, 200, and 400 fs for sheet electron density $N_s = 3.5 \times 10^{11}$ cm^{-2}. The results obtained by taking into account only *e-e* scattering (*e-e* only) are compared with the results that also include electron-phonon interaction at $T = 77$ and 300 K. Solid curves are for the spin-randomized electron gas, dashed curves are for the spin-polarized electron gas. Occupation numbers at each time instant are compared with a quasiequilibrium Fermi-distribution function which is labeled *F*.

weaker in near-band-gap excitation conditions[4,5] at 300 K. At $T=77$ K, the optical-phonon absorption is negligible, while the optical-phonon emission causes the filling of low-energy states with progressing time. Nevertheless, for $t \leq 200$ fs, the thermalization is governed mainly by *e-e* scattering and the difference between the thermalization rates of the SP and SR distribution is attributable to exchange effect.

From Fig. 3 one also sees that the SP gas relaxes to a more degenerate Fermi distribution than the SR gas. Since both gases relax to different Fermi distributions at the same sheet density, it may seem rather problematic to ascribe the differences between the nonequilibrium distributions to exchange *e-e* scattering. Figures 1 and 2, however, show that the exchange is a main source of the differences between the distributions when only *e-e* scattering is operative and, based on Fig. 3, this remains valid also in the presence of the electron-phonon interaction during the first 200 fs.

This section has three main results. (1) Exchange effects tend to deccelerate the thermalization of the electron gas, when the gas density increases. (2) Exchange effects are extremely important in the dense SP electron gas. (3) They are much weaker in the dense SR electron gas, but they should also be taken into account (compare the solid curves in Figs. 1 and 2). After the original submission of this paper, Collet[24] and Snoke[29] reported on the thermalization of the SR gas in bulk GaAs. Snoke argued analytically that the contribution of the exchange term is negligible when the screening is weak, i.e., when the electron density is low (see also Ref. 16). Collet calculated numerically the *e-e* scattering rate for a fixed initial Gaussian distribution. He found that exchange significantly decreases the *e-e* scattering rate at high densities, but its effect is small at low densities. These results are in general agreement with our present work. We have, however, preferred to calculate the time development of the distribution because this is observed experimentally[4,5] (additionally, the scattering rate varies during the thermalization because the distribution is not fixed).

IV. EXCHANGE EFFECTS IN THE *e-h* PLASMA

According to the discussion from the preceding section, for a direct detection of exchange effects one needs to excite high electron densities and to compare the thermalizations of the SR and SP electron gases. Direct observation of nonthermal SR electron distribution was recently reported[30] for *p*-type GaAs, but an application of the measurement technique to the detection of the exchange seems to be problematic (low electron densities were probed through electron-acceptor luminescence).

In the pump-probe experiments of Knox *et al.*, nonthermal distributions of the SR electrons and holes were observed in highly excited GaAs quantum wells[5] and the measurement technique was recently applied to the observation of nonthermal distributions of SP carriers.[20] In this section, we would like to argue that a proper combination of the mentioned pump-probe experiments could, in principle, provide a direct detection of the exchange.

SR carriers are excited and probed by linearly polarized pump and probe pulses,[4,5] while SP carriers have to be excited by circularly polarized pump pulse.[20] Absorption of right-circularly polarized light in GaAs (Ref. 31) excites electrons of spin $-\frac{1}{2}$ from $-\frac{3}{2}$ heavy-hole states and electrons of spin $\frac{1}{2}$ from $-\frac{1}{2}$ light-hole states. These transitions, having relative strength of 3 and 1 (Ref. 32) provide partially SP electron gas. Fully SP electron gas can be created in GaAs quantum wells[32] by matching the excitation laser wavelength to the heavy-hole electron transition energy and suppressing, therefore, the light-hole electron transitions due to the energy splitting of the heavy-hole and the light-hole levels. After right (left) -circularly polarized photoexcitation, the population of carriers with spins up (down) along the direction of the light propagation is created. Since the relaxation time necessary to randomize the orientation of spins is 10^1-10^2 ps (Refs. 32 and 33), it is possible to neglect the spin-relaxation process at least during first 400 fs when the fast thermalization of the energy distribution takes place.

Problems arise from the fact that the *e-h* plasma is excited instead of the isolated electron gas. The observed time-dependent differential transmission[5,20]

$$\Delta T(\hbar\omega,t)/T_0 \propto f_e(\varepsilon_e(\mathbf{k}),t)+f_h(\varepsilon_h(\mathbf{k}),t)\ , \tag{17}$$

does not allow one to distinguish the electron distribution $f_e(\varepsilon_e)$ from the heavy-hole distribution $f_h(\varepsilon_h)$ and the dynamics of electrons and holes is affected by the *e-h* interactions. Thus one should study exchange in the interacting *e-h* plasma.

Figure 4 shows the time evolution of the energy distributions of electrons f_e and holes f_h, normalized like occupation numbers. Also shown is the transient differential transmission $f_e(\varepsilon_e(\mathbf{k}))+f_h(\varepsilon_h(\mathbf{k}))$ versus energy $\varepsilon_e(\mathbf{k})+\varepsilon_h(\mathbf{k})$, which corresponds to the excess energy of the probe photon.[4,5] The upper row shows the results for the SR plasma, the lower row the results for the SP plasma. One sees that the relaxation of f_e+f_h is much slower for the SP plasma. To clarify the origin of this effect, in Fig. 5 we present the thermalization of the plasma without the exchange *e-e* and *h-h* scattering. Compared with Fig. 4, the thermalization of the SP plasma is now much faster, while the thermalization of the SR plasma is only slightly faster. This demonstrates that the exchange significantly weakens the efficiency of the direct *e-e* and *h-h* collisions especially in the SP *e-h* plasma. However, performing the calculations from Figs. 4 and 5 for $N_s=2\times10^{10}$ cm^{-2}, we found almost the same thermalization for the SP and SR plasmas with exchange as well as without exchange. This implies that exchange effects are only important in the dense plasma. All these findings are similar to those for a dense electron gas (Sec. III), because exchange *h-h* scattering manifests itself even more clearly than exchange *e-e* scattering (note the very slow thermalization of the SP hole distribution in Fig. 4) and the *e-h* scattering does not mask the differences due to the exchange.

The thermalization without exchange (Fig. 5) is still slightly slower for the f_e+f_h spectrum of the SP plasma.

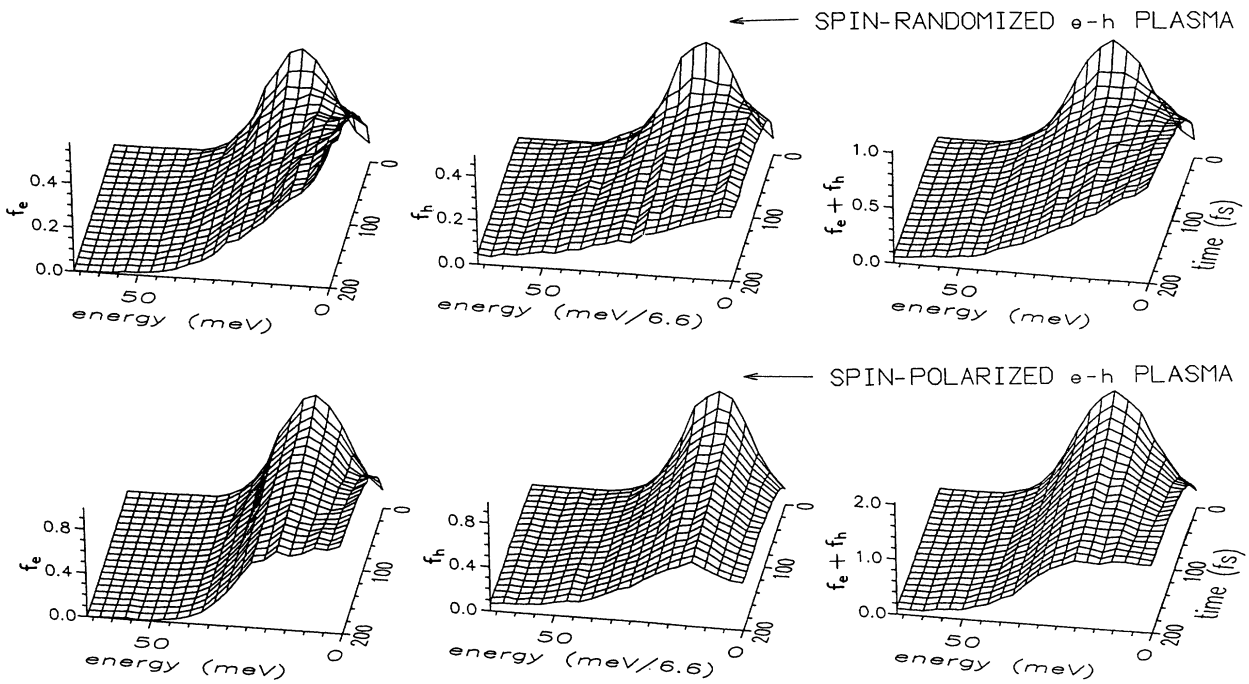

FIG. 4. Time evolution of the energy distribution of electrons (f_e) and holes (f_h). Also shown is the transient differential transmission $f_e(\varepsilon_e(\mathbf{k}))+f_h(\varepsilon_h(\mathbf{k}))$ vs energy $\varepsilon_e(\mathbf{k})+\varepsilon_h(\mathbf{k})$, which corresponds to the excess energy of the probe photon. The results in the upper (lower) row are for the spin-randomized (spin-polarized) *e-h* plasma. The sheet density and the number of simulated *e-h* pairs are $N_s=3\times10^{11}$ cm^{-2} and $N=14\,400$, respectively. The MC time step Δ_t is 5 fs. At $t=0$, distributions f_e and f_h are of Gaussian shape with the half widths 8.7 and 1.3 meV, centered at 17.4 and 2.6 meV, respectively. Both carrier-carrier and carrier-phonon interactions (at lattice temperature of 77 K) were considered. Exchange scattering is taken into account.

This is mainly due to the slower thermalization of the SP electron gas, which is subjected to a stronger Pauli blocking of final states after the *e-e* and *e-h* collisions than the SR electron gas.

Now we wish to point out one difficulty. It is in principle possible[34] to excite initial condition $\max(f_e+f_h)=1$, as used in Figs. 4 and 5 for the SR plasma. For $f_e+f_h>1$ the absorption coefficient becomes negative and a direct band to band absorption does now allow excitation of $f_e+f_h>1$ (Ref. 34), as used for the SP plasma. Therefore, to avoid $f_e+f_h>1$ and to keep the same initial conditions for the SR and SP distributions, calculations from Fig. 4 were repeated for two times lower N_s. As shown in Fig. 6, exchange still decelerates the thermalization of the SP plasma in comparison with the SR one, although the difference is now not so remarkable. When the exchange is omitted, differences between the f_e+f_h spectra become negligible (see Fig. 7).

In Fig. 8 we show again the thermalization for $N_s=3\times10^{11}$ cm^{-2}, but for much broader initial distributions than in Fig. 4 in order to avoid $f_e+f_h>1$. Exchange manifests itself in a similar way, but the thermalization is now much faster. This is due to the enhanced emission of optical phonons by electrons and also due to the fact that the initial distributions are not so far from the thermalized ones as in Fig. 4. As in previous cases, the difference between the f_e+f_h spectra becomes very small, when the exchange is omitted (see Fig. 9).

Comparison of Figs. 4 and 8 shows that the width and center position of the initial distributions strongly affect

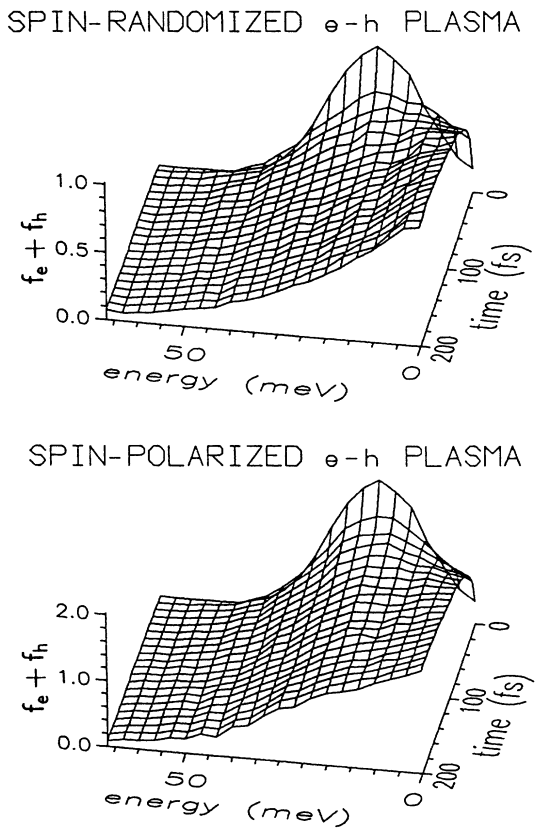

FIG. 5. The same spectra as in Fig. 4, but without exchange scattering.

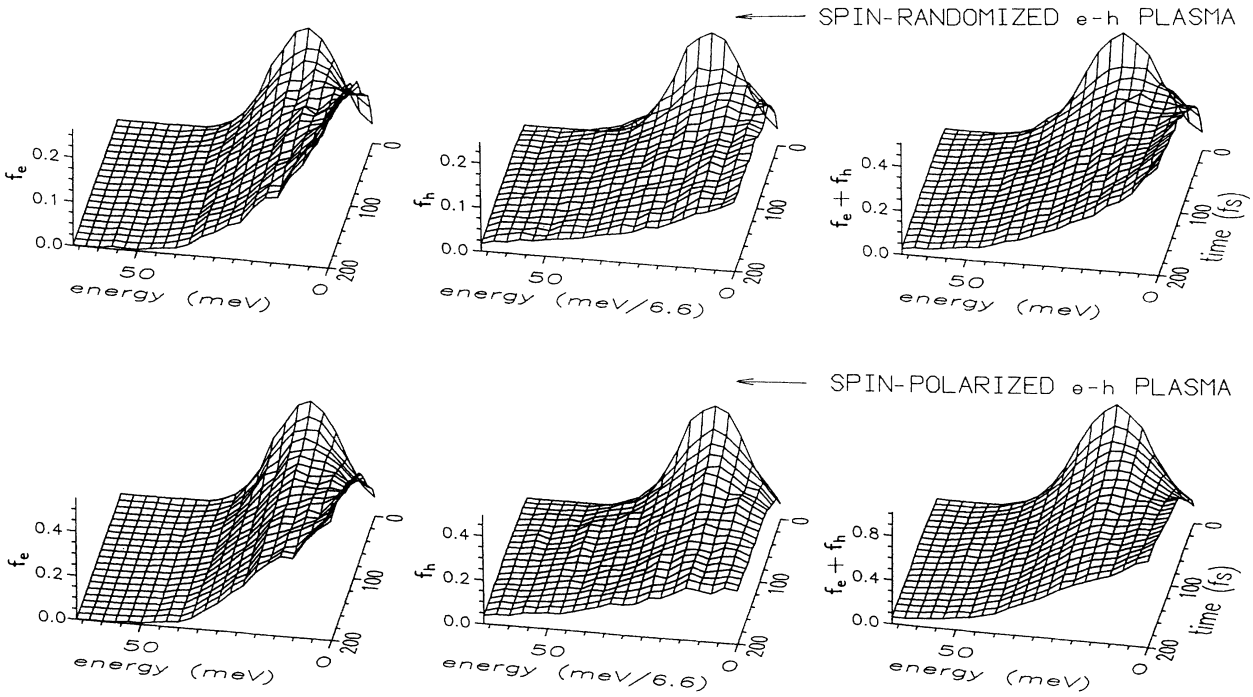

FIG. 6. The same as in Fig. 4, but for $N_s = 1.5 \times 10^{11}$ cm^{-2}.

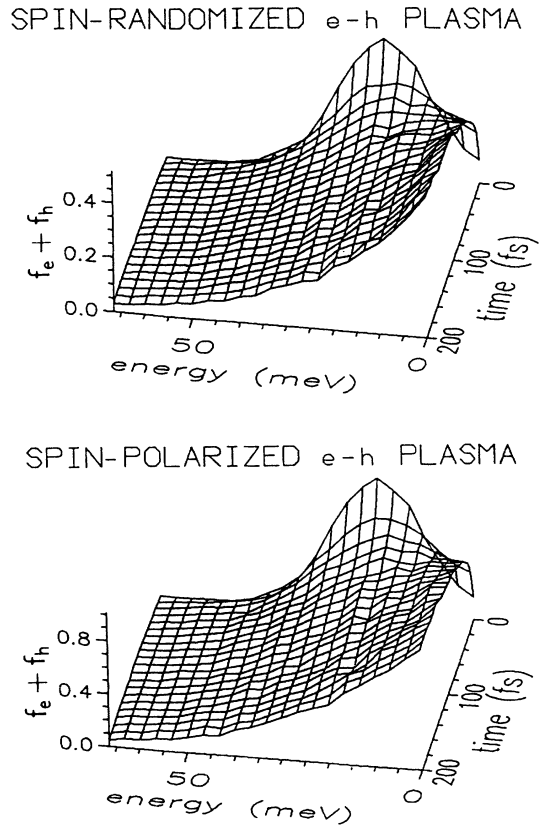

FIG. 7. The same spectra as in Fig. 6, but without exchange scattering.

the thermalization rate. It is, therefore, clear that the initial energy distributions of the SP and SR plasmas have to be quite close, otherwise the observed differences between the thermalizations could not be ascribed only to the exchange effects. The question of how to prepare the same initial distributions (distributions at the end of the photoexcitation) experimentally is not addressed in this paper. Finite duration of the laser pulse [50–100 fs (Refs. 4 and 5)] and coherence effects[35] should be taken into account to solve this problem theoretically. We hope that in the experiment the problem could be solved by experience. The initial distributions and sheet densities, used in Figs. 6 and 8, can be considered as reasonable limits in which the exchange could be detected. Our calculation can, in principle, be extended to much higher excitation energies, but fully SP carriers could not be prepared for such experimental conditions. Low excitation energies of the carriers are also necessary for carrier-carrier scattering to be the dominant scattering process.

V. CONCLUDING REMARKS

In summary, we have included exchange effects into the MC simulation of 2D carrier-carrier scattering. The thermalization of the SP *e-h* plasma, excited close to the band gap of the intrinsic GaAs quantum well, has been compared with the thermalization of the SR one. Due to the exchange *e-e* and *h-h* scattering, the SP plasma is found to thermalize much slower, when the plasma density is greater than about 10^{11} cm^{-3}. With decreasing den-

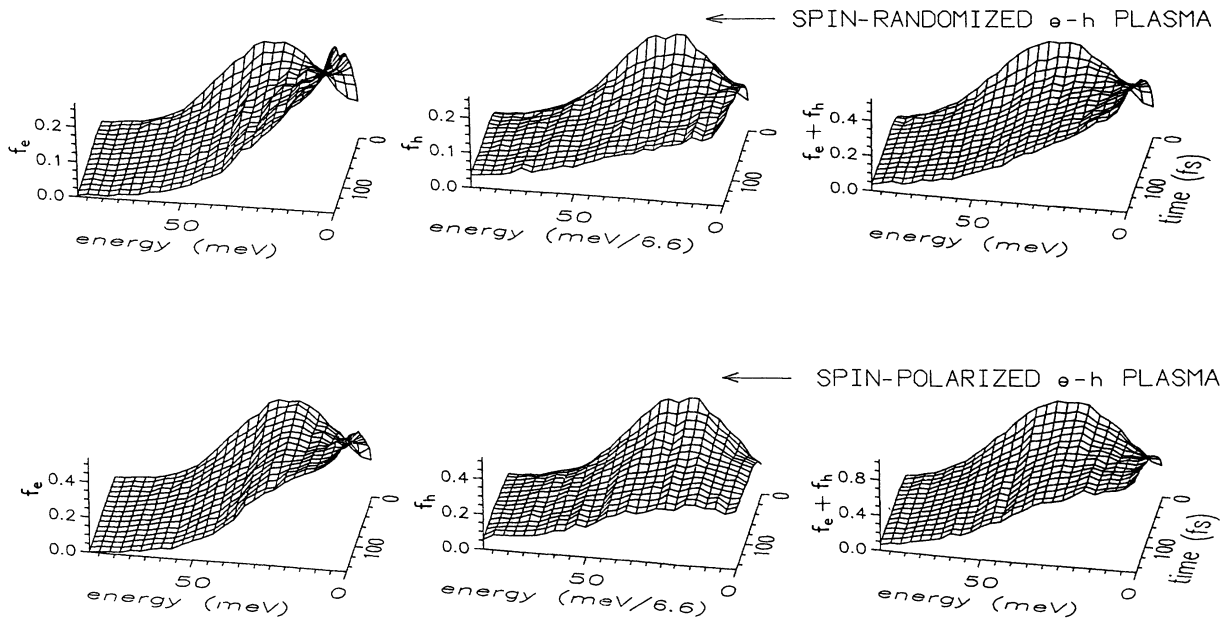

FIG. 8. The same as in Fig. 4, but for two times broader initial distributions with 1.5 times larger excitation energies. $N=35\,000$ and $\Delta_t=2.5$ fs.

sity the effect of exchange as well as the difference between the thermalizations tend to disappear.

We discuss a chance to detect the exchange by comparative measurements of the thermalization of the SP and SR plasmas. Differential transmission spectra obtained using circularly polarized pump and probe pulses[20] should keep a nonthermal "Gaussian" peak for a much longer time than spectra from linearly polarized laser excitation,[5] when the density of photoexcited carriers is high.

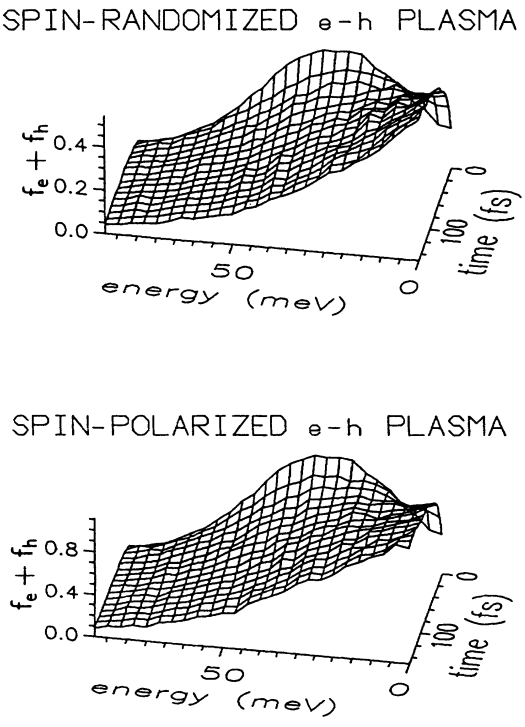

FIG. 9. The same spectra as in Fig. 8, but without exchange scattering.

Slower thermalization of SP photocarriers should be accompanied by a corresponding increase of the time delay of exciton bleaching, which is mainly due to screening and phase space filling by photocarriers at $k=0$.[5,20] Of course, one cannot exclude at present that some additional effects will overlay the effects due to the exchange. Nevertheless, quantitative importance of the exchange for the interpretation of real experiments seems to be obvious from our analysis.

Finally, we wish to point out the simplicity of present MC analysis of the exchange when compared with Boltzmann equation formulations by Collet and Ahmand[34] and Collet.[24] Collet[24] pointed out enormous difficulties in treating dynamic screening and exchange simultaneously. This should be achievable relatively easily in the MC simulation by unifying the recent MC approach to the dynamic screening[12] with the present MC approach to the exchange.

ACKNOWLEDGMENTS

One of the authors (M.M.) would like to thank Dr. Danielle Hulin for useful discussions about femtosecond pump-probe spectroscopy. The work has been supported by the Slovak Grant Agency for Science (GAV No. 2/999187/92).

[1]B. K. Ridley, *Quantum Processes in Semiconductors* (Clarendon, Oxford, 1982).
[2]C. J. Hearn, in *The Physics of Nonlinear Transport in Semiconductors,* edited by D. K. Ferry, J. R. Barker, and C. Jacoboni (Plenum, New York, 1980), pp. 153–166.
[3]J. L. Oudar, D. Hulin, A. Migus, A. Antonetti, and F. Alexandre, Phys. Rev. Lett. **55**, 2074 (1985).
[4]W. H. Knox, C. Hirliman, D. A. B. Miller, J. Shah, D. S. Chemla, and C. V. Shank, Phys. Rev. Lett. **56**, 1191 (1986).
[5]W. H. Knox, D. S. Chemla, G. Livescu, J. E. Cunningham, and J. E. Henry, Phys. Rev. Lett. **61**, 1290 (1988).
[6]S. M. Goodnick, P. Lugli, W. H. Knox, and D. S. Chemla, Solid State Electron. **32**, 1737 (1989).
[7]M. Artaki and K. Hess, Phys. Rev. B **37**, 2933 (1988).
[8]D. Bailey, M. Artaki, C. Stanton, and K. Hess, J. Appl. Phys. **62**, 4639 (1987).
[9]C. J. Stanton, D. W. Bailey, and K. Hess, IEEE J. Quantum Electron. **24**, 1614 (1988).
[10]C. J. Stanton, D. W. Bailey, and K. Hess, Phys. Rev. Lett. **65**, 231 (1990).
[11]D. W. Bailey, C. J. Stanton, and K. Hess, Phys. Rev. B **42**, 3423 (1990).
[12]K. ElSayed and H. Haug, Phys. Status Solidi B **173**, 189 (1992).
[13]M. A. Osman and D. K. Ferry, Phys. Rev. B **36**, 6018 (1987).
[14]S. M. Goodnick and P. Lugli, Phys. Rev. B **37**, 2578 (1988).
[15]M. Moško and A. Mošková, Phys. Rev. B **44**, 10 794 (1991).
[16]N. S. Wingreen and M. Combescot, Phys. Rev. B **40**, 3191 (1989).
[17]A. M. Kriman, M. J. Kann, D. K. Ferry, and R. P. Joshi, Phys. Rev. Lett. **65**, 1619 (1990).
[18]R. P. Joshi, A. M. Kriman, M. J. Kann, and D. K. Ferry, Appl. Phys. Lett. **58**, 2369 (1991).
[19]M. Moško, V. Cambel, and A. Mošková, Phys. Rev. B **46**, 5012 (1992).
[20]J. B. Stark, W. H. Knox, and D. S. Chemla, Phys. Rev. Lett. **68**, 3080 (1992).
[21]K. Yokoyama and K. Hess, Phys. Rev. B **33**, 5595 (1986).
[22]J. F. Young, P. Kelly, and N. L. Henry, Phys. Rev. B **36**, 4535 (1987).
[23]A. Mošková, thesis, Comenius University, Bratislava, Slovakia, 1992.
[24]J. H. Collet, Phys. Rev. B **47**, 10 279 (1993).
[25]S. M. Goodnick and P. Lugli, Phys. Rev. B **38**, 10 135 (1988).
[26]Screening function (10) is valid for strictly 2D electron and hole gases. A more precise formula, which includes a finite width of the 2D gas, can be obtained from (10) by multiplying the second and third terms on the right-hand side of (10) by the form factor $H(Q)$ [see, e.g., G. Zandler *et al.*, in *Proceedings of the 20th International Conference on the Physics of the Semiconductors,* edited by E. M. Anastassakis and J. H. Joaunopoulos (World Scientific, Singapore, 1990), pp. 1146–1149].
[27]L. Rota and D. K. Ferry, Appl. Phys. Lett. **62**, 2883 (1993).
[28]C. Jacoboni and P. Lugli, in *The Monte Carlo Method for Semiconductor Device Simulation,* edited by S. Selberheer (Springer-Verlag, Wien, 1989).
[29]D. W. Snoke, Phys. Rev. B **47**, 13 346 (1993).
[30]D. W. Snoke, W. W. Rühle, Y.-C. Lu, and E. Bauser, Phys. Rev. Lett. **68**, 990 (1993).
[31]G. Lampel, Phys. Rev. Lett. **20**, 491 (1968).
[32]A. Tackeuchi, S. Muto, T. Inata, and T. Fujii, Appl. Phys. Lett. **58**, 2369 (1991).
[33]T. C. Damen, L. Viña, J. E. Cunningham, J. Shah, and L. J. Sham, Phys. Rev. Lett. **67**, 3432 (1991).
[34]J. H. Collet and T. Ahmand, J. Phys. Chem. Solids **47**, 153 (1986).
[35]C. J. Stanton, A. V. Kuznetsov, and Ch. S. Kim, Semicond. Sci. Technol. (to be published).